Chapter 7

Validation of Mechanical Hypothesis of hip Arthritis Development by HIPSTRESS Method

Veronika Kralj-Iglič

Additional information is available at the end of the chapter

http://dx.doi.org/10.5772/59976

1. Introduction

Hip joint connects the upper part of the body to the lower limb. As in human (a bipodal) the motion derives from periodical extension of lower limbs, the one-limb support is a common body position attained in everyday life. Keeping the body in balance and performing the required activities by means of attaining particular body positions or motions and by activating particular muscles is the main function of the hip joint. When the load is transmitted to the supporting leg, the hip bears the body weight (aside from the weight of the supporting leg). Besides the weight the joint is affected also by forces exerted by the surrounding tissues (e.g. muscles, tendons, ligaments and fluids). As the human body is subject to laws of physics, it is therefore indicated that mechanical parameters such as forces and stresses can be connected to physiological and patophysiological processes in the hip joint.

Understanding of causes of the effects on development of the body was dramatically accelerated by the discovery of X-rays in 1895, which enabled imaging of inner body structures without cutting them. It was found that the lateral coverage of the femoral head with the acetabulum is an important parameter in predicting the development of hip cartilage degeneration and hip osteoarthritis [1]. Besides providing new diagnostic technologies, physical methods contributed also to revealing mechanisms of disease development. According to the mechanical hypothesis, too high load of the hip was empirically considered as a cause for deterioration of the hip joint.

2. Hip stress as a relevant biomechanical parameter

Poor lateral coverage of the femoral head by the acetabulum was connected to smaller load bearing area and therefore larger contact stress on the hip cartilage and bones. To increase the

load bearing area and prevent early hip osteoarthritis, various operative techniques were suggested [2-9]. In these operations the load bearing area was increased by increasing the lateral coverage of the femoral head by the acetabular roof. However, proof for the mechanical hypothesis stating that unfavorable distribution of stress in the hip is connected to early hip osteoarthritis, requires a method for assessment of hip stress.

Hip stress was measured in vitro and in vivo by using different techniques (e.g. pressure sensitive film and instrumented prothesis) [10]. After a thorough study involving development of a special Austin Moore partial endoprothesis and its validation in vitro, a specimen was implanted into a patient [11]. Contact hip stress was recorded by electromagnetic signal deriving from piezoelectric transducers on the head of the prothesis. The signal was recorded by a coil placed arround the patient's thigh. The location of the particular transducer was distinguished by the frequency of the signal. The patient was followed during the rehabilitation and in different activities for several years. Measurements recorded nonuniform distribution of hip stress over the load bearing area. Peak stresses as high as 15 MPa were recorded in everyday activities (e.g. standing up from a cca 25 cm chair).

To assess biomechanical parameters, theoretical models were developed. Finite element method was used to predict stresses within hip bones [12]. According to this method the hip is imagined as composed of small elements which act one upon another according to laws of elastomechanics. Two dimensional and three dimensional models were elaborated. Taking into account the materials elastic constants, the relevant constraints and the load on the hip the values of stress subject to each element can be calculated. Calculation requires solving large systems of equations which became possible by development of powerful computers. Important general knowledge was obtained by this method as for example the effect of the bone stiffening and cartilage elastic modulus on the stress values and distribution. Dynamic effects were studied by measurements of the effect of the movement on the piezoelectric force plate and by recording the motion of the subject by the video camera in combination with mathematical model [13]. In the model, the body was divided into segments connected by joints. Muscle and tendon mechanics was taken into account. Resultant joint forces were calculated from intersegmental forces by solving the inverse dynamics problem.

However, these methods were not appropriate for clinical studies where large number of hips should be assessed within reasonable time and possibilities. Also, the elastic constants of the material composing hip and pelvis for a particular person are largely unknown. For clinical studies of disease specificity, analytically or almost analytically solvable models based on the individual hip geometry were found more appropriate [14-16]. The strength of these methods lies in appropriate abstractions and choices of a small number of relevant features that render the model simple enough to be transparent with respect to the effect of the parameters. Development of such methods enabled analysis of large populations of hips with different pathologies. The mechanical hypothesis claiming that elevated contact hip stress is a possible cause of hip osteoarthritis was tested on a large cohort of hips with idiopathic osteoarthrosis and compared to a population of »normal« hips [16]. It was found that »compressive stress is of minor importance with respect to the etiology of idiopathic osteoarthrosis of the hip joint«. The results of this thorough study seemed decisive and discouraging for further questioning

http://dx.doi.org/10.5772/59976

the mechanical hypotehsis as regards osteoarthritis, but the effect of stress was further investigated by determination of stress in patients with congenital dislocation of te hip [17,18]. It was found that an integral of stress over time statistically significantly correlated with clinical status [18] and that the values of stress beyond a threshold of 2MPa and integrated stress beyond threshold of 10MPa-years were connected to poor clinical outcome [17].

3. Method HIPSTRESS

Method HIPSTRESS was intended for analyses of large populations of hips. Its use is simple enough to be used by medical doctors and it requires some minutes to assess biomechanical parameters if the geometrical parameters of hips are known. The method consists of two mathematical models, one for determination of the resultant hip force in one legged stance [19] and the other for determination of contact hip stress distribution [20]. Both methods introduced some improvements with respect to previously developed models.

3.1. Model HIPSTRESS for resultant hip force

The model for the resultant hip force [19] considers the body to be composed of two segments: the lower segment (the loaded leg) and the upper segment (the rest of the body). The static equilibrium requires that the resultant of all external forces acting on each segment is zero and that the resultant of all external torques acting on each segment is zero. For the upper segment this requirement is

$$\left(\mathbf{W}_{\mathrm{B}} - \mathbf{W}_{\mathrm{L}}\right) + \sum \mathbf{F}_i - \mathbf{R} = 0, \tag{1}$$

$$\mathbf{a} \times \left(\mathbf{W}_{\mathrm{B}} - \mathbf{W}_{\mathrm{L}}\right) + \sum \mathbf{r}_i \times \mathbf{F}_i = 0, \tag{2}$$

where $\mathbf{W}_{\mathrm{L}}$ is the weight of the loaded leg, $\mathbf{W}_{\mathrm{B}}$ is the body weight, $\mathbf{F}_i$ are forces of muscles that are active in the one-legged stance, $\mathbf{R}$ is the resultant hip force, $\mathbf{a}$ is the vector to the center of the mass of the body without the loaded leg and $\mathbf{r}_i$ are vectors to the origins of the muscle forces. The coordinate system for the upper body segment was chosen at the origin of the resultant hip force (the center of the feomral head) and therefore the torque due to this force is 0. The index i runs over all included muscles.

For the upper body segment, forces of 9 effective muscles are taken into account. Muscle forces are considered to act in straight lines between the muscle attachment points. The muscles that attach in larger areas were represented by several effective muscles. The effective muscles included in the model are gluteus minimus anterior, gluteus minimus middle, gluteus minimus posterior, gluteus medius anterior, gluteus medius middle, gluteus medius posterior, tensor fasciae lateae, piriformis and rectus femoris. The force of each muscle $\mathbf{F}_i$ was considered proportional to the muscle cross section area A_i and average tension in the muscle f_i,

$$\mathbf{F}_i = f_i A_i \left(\mathbf{r}_i - \mathbf{r}'_i\right) \Big/ \left|\left(\mathbf{r}_i - \mathbf{r}'_i\right)\right|, \; i = 1,2,3,...,9. \tag{3}$$

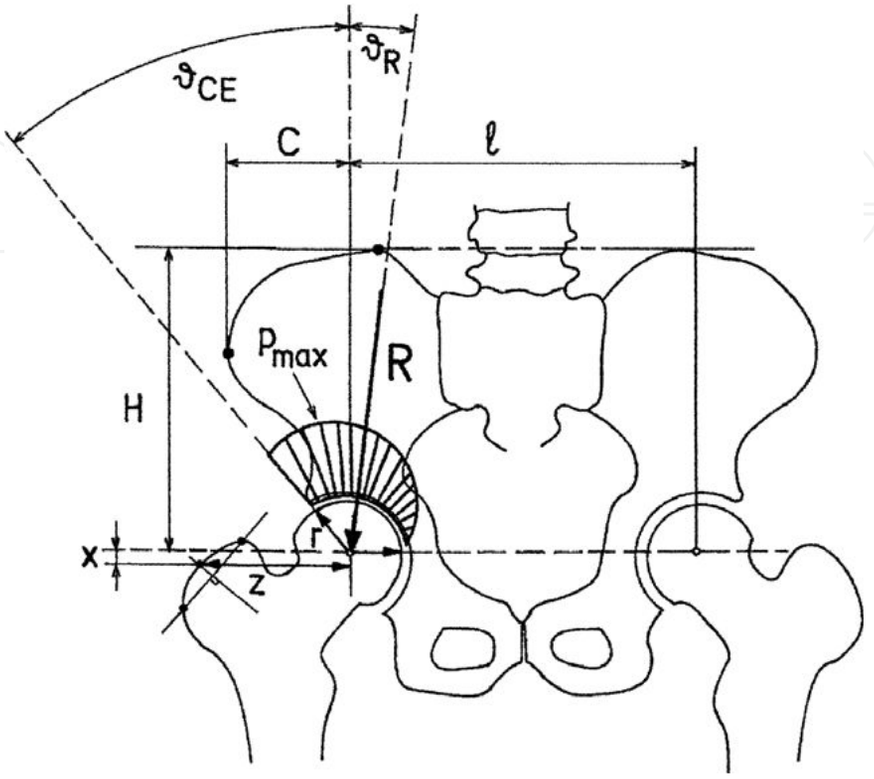

Figure 1. Geometrical parameters of the hip and pelvis for the HIPSTRESS method, resultant hip force and hip stress distribution. From [23].

The forces and the torques have three dimensions, therefore the model consists of six equations (3 for equilibrium of forces and 3 for equilibrium of torques). For known origin and insertion points of the muscles, and known cross section areas the unknown quantities are the muscle tensions and three components of the resultant hip force **R**. Since there are 9 effective muscles and 3 components of the force **R,** there are 12 unknowns and 6 equations. To solve this problem, a simplification was introduced by dividing the muscles into three groups (anterior, middle, posterior) with respect to the position. It was assumed that the muscles in the same group have the same tension. This reduced the number of unknowns to 6 as required for solution of the complex of 6 equations. The muscle origin and insertion points and the muscle cross-section were taken from [21] and [22], respectively. The geometry of the individual patient was taken into account by correction of muscle attachment points according to the geometrical parameters obtained from the standard anteroposterior radiograph (the interhip distance (*l*), the height (*H*) and the width (*C*) of the pelvis, and the position on the greater trochanter relative to the centre of the femoral head (*x*,*z*)).

Results obtained with the HIPSTRESS model for resultant hip force showed that the force lies almost in the frontal plane of the body through both femoral heads. To further simplify the

http://dx.doi.org/10.5772/59976

calculations it was assumed in most studies that the force lies in the frontal plane and is represented by its magnitude R and its inclination with respect to the vertical ϑ_R.

3.2. Model HIPSTRESS for contact hip stress

Model for contact hip stress was thorougly described in a previous contribution [24] and will be only briefly described here. Femoral head is represented by a part of the sphere and acetabulum is represented by a part of the spherical shell. Articular spehere represents both, the acetabular sphere and the femoral head sphere. When unloaded, both representative spheres have the same origin. Between the spheres there is an elastic continuum representing cartilage. The cartilage is subject to Hooke's law. When loaded, the origin of the femoral head sphere is slightly displaced with respect to the acetabular sphere and the cartilage is squeezed. It is assumed that stress is proportional to displacement. Some points on the femoral head are moved closer to the acetabulum and some points are moved away from the acetabulum. The stress pole is the point on the articular sphere that corresponds to the closest approach of the femoral head and the acetabulum spheres. It is assumed that there is no friction in the tangential direction to the spherical surface, so the normal stress is the only relevant stress acting in the hip.

The base of the mathematical model is the cosine dependence of contact stress on the space angle between the position of the stress pole and the chosen point on the articular surface γ [16],

$$p = p_0 \cos \gamma \ , \tag{4}$$

where p_0 is the value of stress at the pole. The essential contribution of the HIPSTRESS model for stress is the elaboration of the load bearing area. The choice of the coordinate system and the definition of the borders of the load bearing area renders the elaborated load bearing area always symmetric, regardless of the direction of the resultant hip force. The lateral boundary of the load bearing area is defined by intersection of the articular sphere and the plane which is inclined with respect to the sagittal plane for ϑ_{CE} (the centre-edge angle of Wiberg). On the medial side the border is defined by the condition that the stress vanishes, i.e. the medial border is for the angle $\pi/2$ allienated from the stress pole. The connection between the resultant hip force and the hip stress distribution

$$\mathbf{R} = \int p \, \mathbf{dA} \ , \tag{5}$$

where the integration is performed over the load bearing area, yields three equations for three unknowns: the angles defining the position of the hip stress pole (Θ and Φ) and the value of stress at the pole p_0 [20,24]

$$\Phi = 0, \ \pi \ , \tag{6}$$

$$\tan\left(\vartheta_R+\Theta\right)=\cos^2\left(\vartheta_{CE}\text{-}\Theta\right)\Big/\left(\pi/2+\vartheta_{CE}-\Theta+\sin\left(2\left(\vartheta_{CE}-\Theta\right)\right)\Big/2\right)\ , \tag{7}$$

$$p_0=\ 3R\sin\left(\vartheta_R+\Theta\right)\Big/2r^2\cos^2\left(\vartheta_{CE}-\Theta\right)\ , \tag{8}$$

where Φ is the azimuth coordinate of the stress pole on the articular surface. To determine stress at any point of the load bearing area, the solution of the nonlinear equation for the coordinate of the pole Θ Eq. (4) should be found. Re-arranging Eq.(7) by substitution [25]

$$\Theta=\boldsymbol{x}-\left(\vartheta_R-\vartheta_{CE}\right)/2 \tag{9}$$

transforms the nonlinear equation (7) into

$$\begin{aligned}&\tan\left(\left(\vartheta_R+\vartheta_{CE}\right)/2+x\right)=\\&=\cos^2\left(\left(\vartheta_R+\vartheta_{CE}\right)/2\text{-}x\right)\Big/\left(\pi/2+\left(\vartheta_R+\vartheta_{CE}\right)/2\text{-}x+\sin\left(2\left(\left(\vartheta_R+\vartheta_{CE}\right)/2\text{-}x\right)\right)/2\right)\ .\end{aligned} \tag{10}$$

It follows from Eq. (10) that the solution of Eq. (7) (i.e. the position of the stress pole depends solely on ($\vartheta_R + \vartheta_{CE}$)).

The integration of Eq.(5) is performed over the load bearing area. Stress is unevenly distributed over the load bearing area. It decreases towards the medial border while on the lateral side there are two possibilities, depending on the position of the hip stress pole. If the pole lies within the load bearing area, stress increases in the medial direction, reaches maximum and then decreases. The pole, being an abstract quantity that reflects the extent and the direction of the relative movement of the femoral head and the acetabulum upon loading, may however lie outside the load bearing area. In this case, stress monotonously decreases towards the medial border. The contact hip stress distribution is represented by the peak value of hip stress on the load bearing area (p_{max}). If the pole lies in the weight bearing area the peak stress is equal to its value at the pole ($p_{max} = p_0$). If the stress pole lies outside the load bearing area, the peak stress is equal to the value of stress at the point of the load bearing area which is closest to the pole. Other parameters that represent stress distribution are the index of the stress gradient at the lateral acetabular rim (G_p)

$$G_p=\text{-}p_0/r\ \cos\vartheta_F \tag{11}$$

where ϑ_F is the functional angle of the load bearing,

$$\vartheta_F=\ \pi/2+\vartheta_{CE}-\Theta \tag{12}$$

http://dx.doi.org/10.5772/59976

and the load bearing A_F

$$A_F = 2r^2 \vartheta_F \ . \tag{13}$$

An example of the stress distribution calculated by HIPSTRESS method is shown in Figure 2. The green line denotes the magnitude of the contact hip stress p in the frontal plane through centres of both articular spheres. The left hip has normal shape. The right hip is considerably deformed as the patient underwent in the childhood the Perthes disease. In the normal (left) hip the stress increases in the medial direction, reaches maximum and then decreases. The functional angle and the load bearing area are large. The pole lies within the load bearing area and the index of hip stress gradient is negative. In the deformed (right) hip the stress monotonously decreases in the medial direction. The functional angle is small. The pole lies outside of the load bearing area and the index of hip stress gradient is positive. However, the load bearing area is not small in the deformed hip as the smaller functional angle is compensated by the larger radius of the articular sphere (Eq. (13)). Consequnetly, the peak stress is almost equal in both hips.

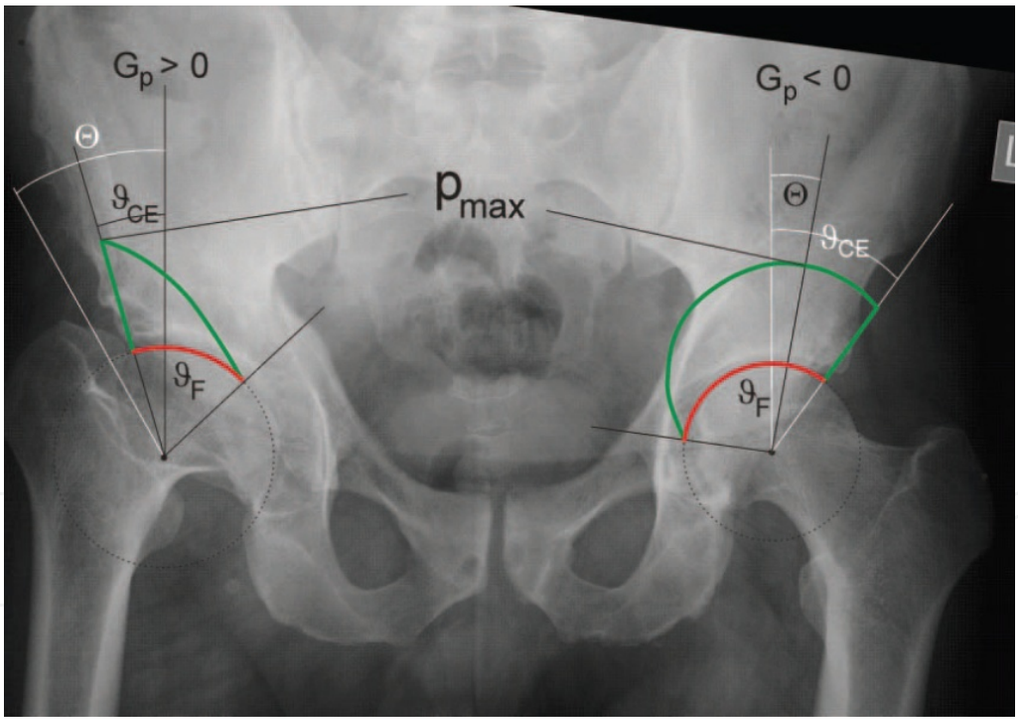

Figure 2. Distribution of hip stress on the load bearing area of a normal hip (left) and a hip after Legg-Calve-Perthes disease (right). The green line represents the magnitude of stress in the frontal plane through the centers of the femoral heads. The red line indicates the functional angle determining the load bearing area. From [26].

Figure 3 shows the peak hip stress (A) and the coordinate of the stress pole (B) in dependence on the sum of the angles ($\vartheta_{CE} + \vartheta_R$). As this sum implies the solution of the system of equations representing the vector equation (5), the two angles can compensate each other. Smaller centre-

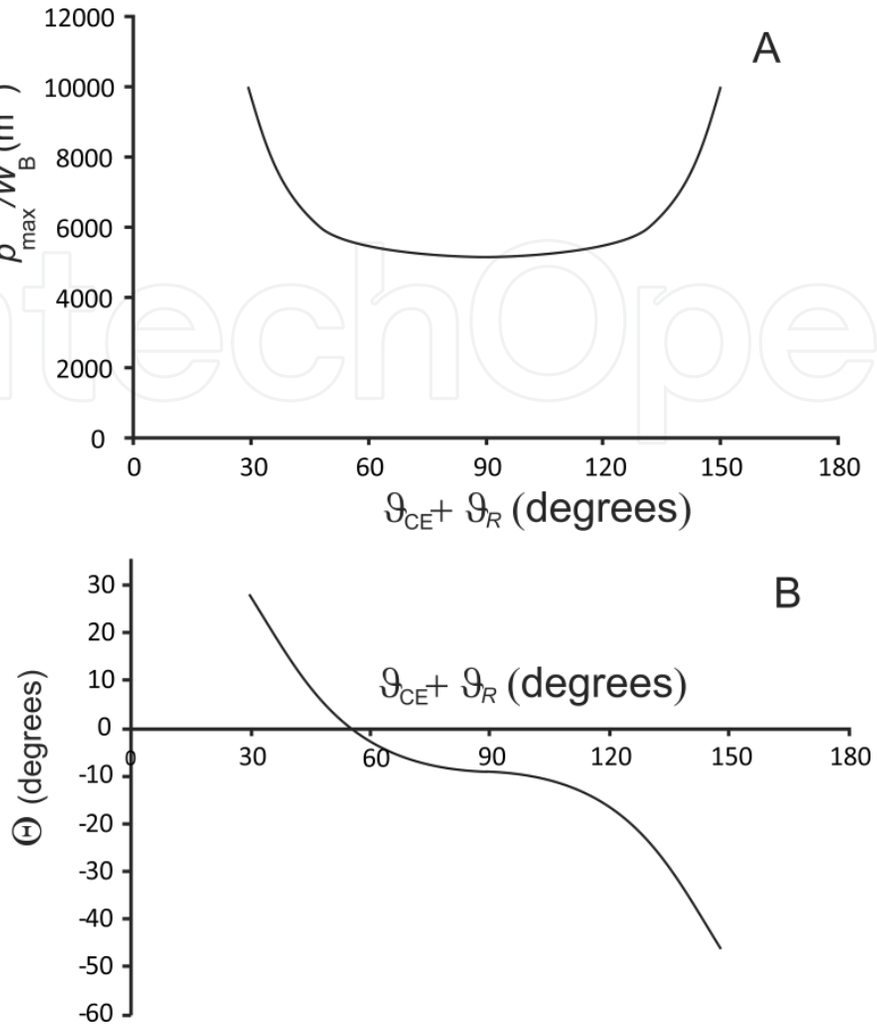

Figure 3. A: Peak contact stress as a function of the parameter ($\vartheta_{CE} + \vartheta_R$). B: position of the stress pole as a function of the parameter ($\vartheta_{CE} + \vartheta_R$). Lines were for a hypothetical hip with $R/W_B = 2.6$ and $r = 1.6$ cm. Adapted from [25].

edge angle can be complemented by larger inclination of the resultant hip force to assure favorably large enough functional angle and load bearing area. It is expected that large centre-edge angle means larger load bearing area and lower stress, but Figure 3 shows that for very large centre-edge angles combined with large inclinations of the resultant hip force, stress increases. Such situation would take place for large centre-edge angles (larger than 70 degrees) since the resultant hip force in the one-legged stance is usually smaller than 20 degrees. The above described model of resultant hip force describes the one-legged stance. The model for stress is general with respect to body position and enables calculation of hip stress distribution if the resultant hip force and some additional geometrical parameters of the hip are known. To obtain stress with the HIPSTRESS model for stress it is therefore not necessary that the resultant hip force is calculated by the HIPSTRESS model for the resultant hip force. The force can also be determined experimentally. However, it is necessary to know additional geometrical parameters such as the centre-edge angle ϑ_{CE} and the radius of the articular sphere r (Figure 1).

http://dx.doi.org/10.5772/59976

4. Computer program and nomograms for determination of the resultant hip force and peak contact stress in the HIPSTRESS method

Computer program was developed to calculate the force **R** (its magnitude and inclination with respect to the vertical direction), the peak hip stress p_{max} and the coordinate Θ of the pole. The program is available at http://physics.fe.uni-lj.si/projects/orthopaedic.htm Also, the nomograms were elaborated [27] for those who do not have a possibility to use the computer. They prove useful also as the rapid development of computer science requires compatibility of the program with hardware and other software which is not always available. The input data of the program HIPSTRESS are the geometrical parameters of the hip and pelvis that can be assessed from images of the hip and pelvis geometry (e.g. X-rays or magnetic resonance) (Figure 1): the interhip distance (l), the pelvic width (C), the pelvic height (H), the coordinates of the effective muscle attachment point on the greater trochanter in the coordinate system of the femur (z and x), the femoral head radius (r) and the centre-edge angle ϑ_{CE}. To determine the resultant hip force and the contact hip stress distribution also the magnitude of the body weight W_B should be known. However, besides the force and the stress, also the parameters normalized with respect to body weight are of interest, R/W_B, p_{max}/W_B and G_p/W_B. These normalized parameters reflect the effect of the hip and pelvis geometry on the force and the stress.

Below we present nomograms for determination of resultant hip force and peak hip stress. The nomograms were calculated by using the computer programs. As there are many parameters that define the model it was not appropriate to consider all possible combinations of parameters but only those that yield the largest effect. The vertical position of the effective muscle attachment point on the greater trochanter was therefore not taken into account. Determination of the force is performed in two steps: determination of the inclination of the resultant hip force and determination of the magnitude of the resultant hip force. In determination of the magnitude, the effect of the pelvic width and height was disregarded as these parameters proved less important than the lateral extension of the greater trochanter and the interhip distance. To assess stress from the nomograms, we choose the $R/W_B(l/2)$ curve (Figure 4) pertaining to the combination of z and $l/2$ closest to the measured values and determine R/W_B. Then we choose the $\vartheta_R(l/2)$ diagram (Figure 5) pertaining to the combination of z, H and C closest to the measured values and determine ϑ_R. Using thus determined R/W_B and ϑ_R, and the measured values of ϑ_{CE} and r we choose the $p_{max}r^2/W_B(\vartheta_{CE}+\vartheta_R)$ diagram pertaining to the relevant interval of $(\vartheta_{CE}+\vartheta_R)$ (Figure 6) and determine $p_{max}r^2/W_B$. To assess p_{max}/W_B we divide the obtained value by r^2. To obtain p_{max} we multiply the obtained value with body weight W_B.

For example, let us determine the resultant hip force and peak hip stress in a hip with parameters $l/2$=9.8 cm, C=5.6 cm, H=15.0 cm, x = 1.0 cm, z = 6.1 cm, r = 2.3 cm, ϑ_{CE} = 32 degrees and W_B=750 N. To assess R/W_B we chose in Figure 4 the curve pertaining to z = 6 cm and obtain for $l/2$ = 10 cm the value R/W_B = 2.7 (see dotted lines in Figure 4). Then we assess ϑ_R. The closest values of the parameters $l/2$, H and z are $l/2$ = 10cm, H =16cm and z = 6 cm while the value of C is between 5

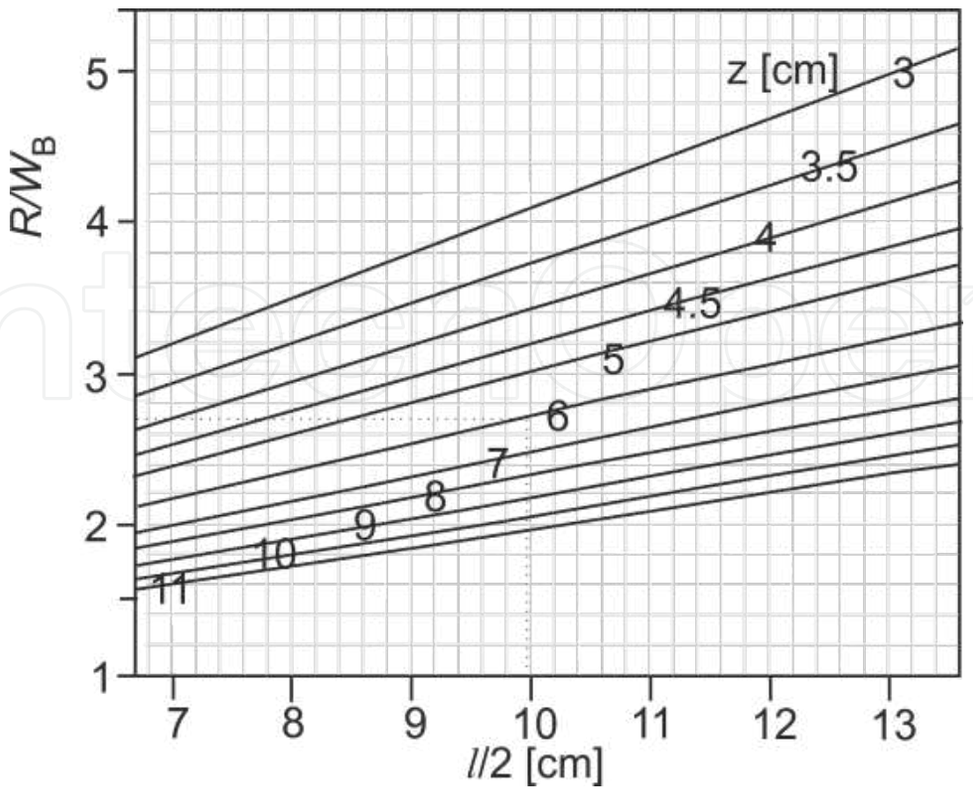

Figure 4. Nomograms for determination of the magnitude of the resultant hip force. The dependence of the magnitude of the force R on half of the interhip distance $l/2$ for different lateral extensions of the greater trochanter z. Adapted from [27].

and 6 cm, therefore we can assess ϑ_R from panels h and k (Figure 5). The value of ϑ_R obtained from panel h (pertaining to C = 5 cm) is 8 degrees and the value of ϑ_R obtained from panel k (pertaining to C = 6cm) is 7 degrees (dotted lines in Figure 5). For C = 5.6 cm we can estimate that ϑ_R = 7.5 cm. Using the obtained values ϑ_R = 7.5 degrees, R/W_B = 2.7 and the geometrical parameters r = 2.3 cm and ϑ_{CE} = 32 degrees we assess $p_{max}r^2/W_B$ from Figure 6 (see dotted lines in Figure 6). The sum (ϑ_{CE}+ϑ_R) is (32+7.5 ≅ 40) degrees, therefore we chose panel c and the curve pertaining to z = 6 cm. The obtained value of $p_{max}r^2/W_B$ is 1.75. Dividing this value by r = 2.3 cm yields p_{max}/W_B =3300 m^{-2}. For W_B=750N the peak stress is finally p_{max}=2.47 MPa.

It can be seen from the nomograms that smaller C and smaller H are biomechanically favorable as they yield larger ϑ_R. As regards ϑ_R, for large z smaller interhip distance is favorable and for smaller z larger interhip distance is more favorable, however, the dependencies are weak. Smaller lateral extension of the greater trochanter z and larger interhip distance l increase the magnitude of resultant hip force R/W_B. Peak hip stress decreases with decreasing (ϑ_{CE} + ϑ_R) up to (ϑ_{CE} + ϑ_R = π/2) and increases with increasing R/W_B [25]. For low hip stress (ϑ_{CE} + ϑ_R) is large enough that the curve $p_{max}r^2/W_B$(ϑ_{CE}+ϑ_R) is almost flat, mostly on the account of large ϑ_{CE}. Thus, the most favorable hip geometry has small interhip distance, large lateral extension of the grater trochanter, small pelvic width and height, large radius of the femoral head and large (but within limits) centre edge angle.

http://dx.doi.org/10.5772/59976

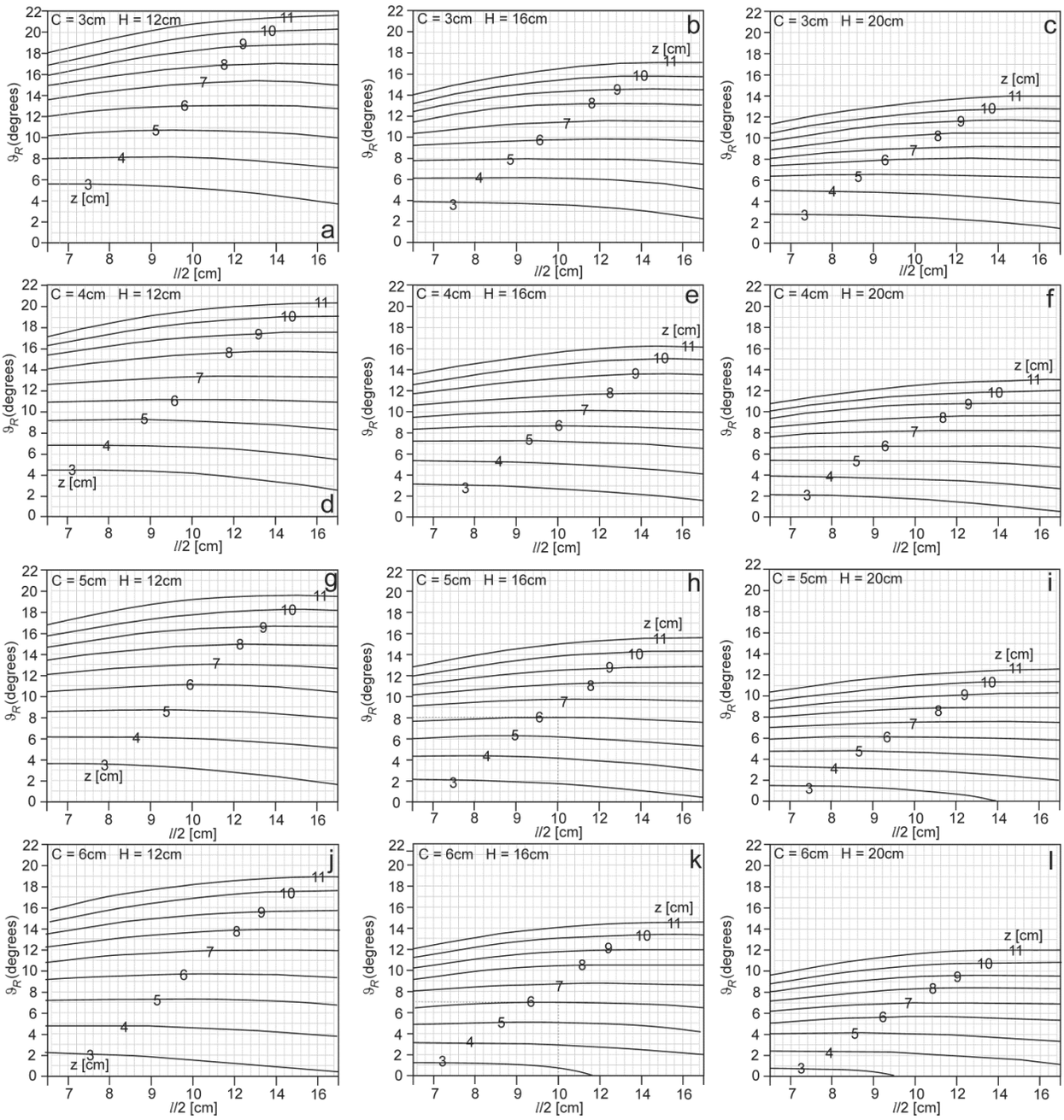

Figure 5. Nomograms for determination of the inclination of the resultant hip force. The dependence of the inclination of the force ϑ_R on half of the interhip distance $l/2$ for different lateral extensions of the greater trochanter z. a: C=3cm, H=12 cm, b: C=3cm, H=16cm, c: C=3cm, H=20 cm, d: C=4cm, H=12 cm, e: C=4 cm, H=16 cm, f: C=4 cm, H=20 cm, g: C=5 cm, H=12 cm, h: C=5 cm, H=16 cm, i: C=5cm, H=20 cm, j: C=6 cm, H=12 cm, k: C=6 cm, H=16 cm, l: C=6 cm, H=20 cm. Adapted from [27].

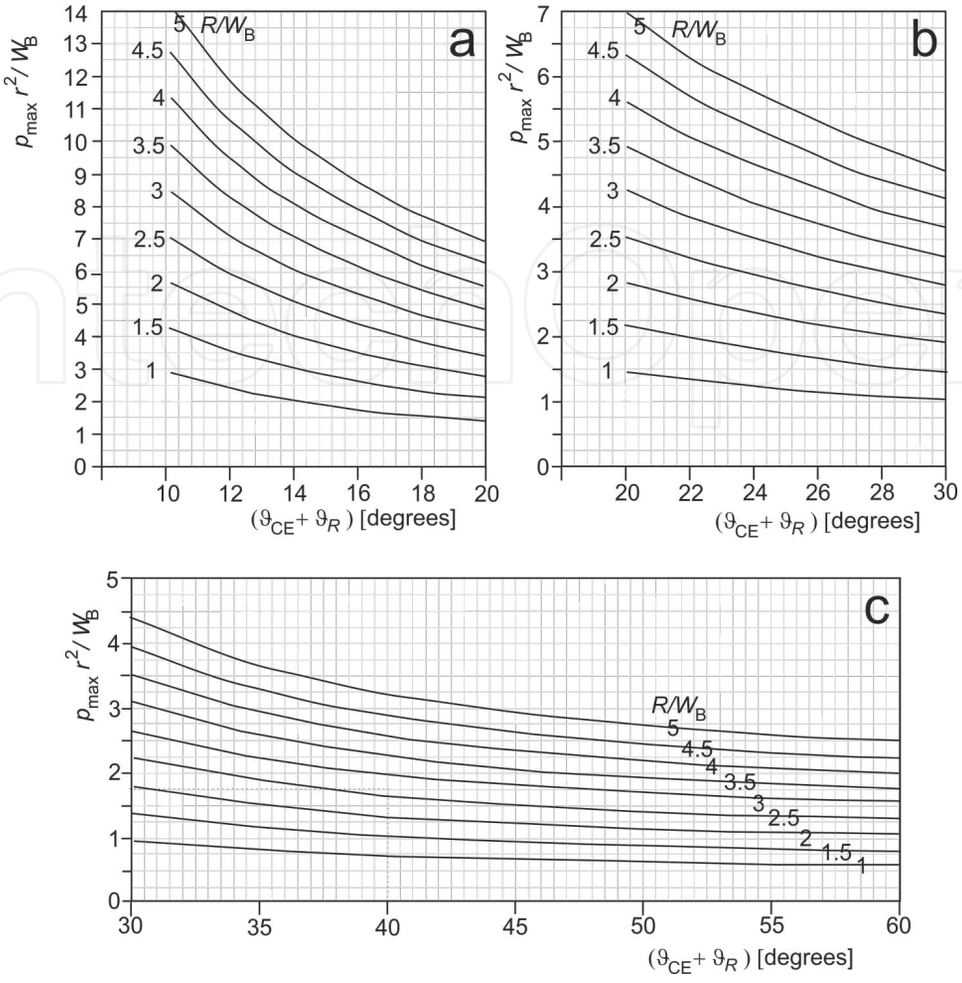

Figure 6. Nomograms for determination of the peak hip stress. The dependence of $p_{max}r^2/W_B$ on the sum of the angles $(\vartheta_{CE}+\vartheta_R)$ for different values of the resultant hip force R/W_B. Due to large variation of the values with $(\vartheta_{CE}+\vartheta_R)$ panel a pertains to the range of $(\vartheta_{CE}+\vartheta_R)$ between 10 and 20 degrees, panel b pertains to the range between 20 and 30 degrees and panel c pertains to the range between 30 and 60 degrees. Adapted from [27].

5. Biomechanical parameters in normal and dysplastic hips

5.1. Comparison between »normal« female and male hips

The early population studies by the HIPSTRESS method considered »normal« hips. Geometrical parameters were assessed from standard anteroposterior radiograms retrieved from the archives. The pictures that showed no abnormalities in the hip region were included in the analysis; the patients had the pictures taken due to back pain. The exclusion criteria for participation in the study were clinical or radiographic signs of hip pathology, insufficient technical quality of the radiograph and incomplete presentation of pelvis on the radiograph. The first clinical study addressed differences between female and male hips [28]. Study of relevant geometrical parameters showed differences between 79 female and 21 male hips (Table 1). Female subjects had considerable and statistically significantly larger interhip

http://dx.doi.org/10.5772/59976

distance and smaller femoral heads than male subjects, which is biomechanically unfavorable as it increases the magnitude of the peak stress. It was suggested that less favorable hip and pelvis geometry as regards hip stress »could be one of the reasons for the increased incidence of arthritis in women« [28]. However, stress was not actually calculated in that study.

	Female (79)	Male (21)	Difference (%)	p
w(cm)	14.05	12.94	8	10^{-4}
H(cm)	15.13	15.42	-2	0.11
C(cm)	6.12	5.47	11	0.07
r(cm)	2.38	2.68	-12	10^{-4}
ϑ_{CE}	37	36.5	1	0.31

Table 1. Median values of the geometrical parameters of 79 female and 21 male »normal« hips as determined in the first HIPSTRESS population study. Parameter w is the distance between the medial acetabular rims.

The differences between parameters (e.g., x) were calculated with respect to the mean value $(x_{female} + x_{male})/2$. The statistical significance of the difference (the probability p) was calculated by using Mann-Whitney test. Instead of the interhip distance l the study considered the distance between the medial acetabular rims w as to avoid the effect of the femoral head size on the interhip distance. Adapted from [28].

5.2. Comparison between »normal« and dysplastic hips

Stress was assessed in a population of dysplastic hips to test the hypothesis that it is higher than in »normal« hips and at the same time test the models [29]. The diagnosis of dysplasia was made on the basis of standard clinical and radiographic evaluation [29]. As it was found in the previous study [28] that female and male hips have considerably different geometrical and biomechanical parameters, the groups of female and male hips were considered separately, however the group of male hips was too small to allow for gender-matched comparison with »normal« hips, therefore the male hips were excluded from the analysis. 47 dysplastic female hips were included in the final analysis. The sample consisted of 20 right and 27 left hips, and the age of the subjects ranged from 18 to 52 years with a median of 33 years. The gender- and age-matched control group consisted of subjects who had had a radiograph taken of the pelvic region for reasons other than degenerative hip disease and in whom the pelvic radiograph had shown no signs of hip pathology. This group consisted of 36 hips, 18 right and 18 left, and the age of the subjects ranged from 18 to 41 years with a median age of 33 years. The results showed considerable and statistically very significant differences in most of geometrical parameters relevant for the HIPSTRESS model, in particular in resultant hip force and in peak contact stress (Table 2). The largest difference (80%) was in the centre-edge angle (Table 2). There was a 65% difference in contact hip stress; small centre-edge angle in dysplastic hips was to some extent compensated by larger radius of the femoral head and more favorable shape of the pelvis (smaller width and height). This study [28] was the first one that clearly

showed on a relatively large cohort that contact hip stress is considerably higher (for about twice) in dysplastic female hips than in »normal« female hips. Also, it provided the first estimate of »normal« stress, i.e. the average value 3100 m^{-2}. It was therefore suggested that the peak contact stress is a suitable parameter to assess risk for development of early arthritis of the hip.

	Dysplastic (47)	Normal (36)	Difference(%)	p
(l ± SD) (cm)	20.8±1.2	19.5±0.9	6	<0.001
(C ± SD) (cm)	4.7±1.0	5.6±1.1	-17	<0.001
(H ± SD) (cm)	14.4±1.3	15.0±1.0	4	0.024
(x ± SD) (cm)	1.4±0.6	1.0±0.5	33	<0.001
(z ± SD) (cm)	5.6±0.6	6.1±0.6	8	<0.001
(r ± SD) (cm)	2.6±0.2	2.3±0.1	12	<0.001
(ϑ_{CE}±SD) (degrees)	13±8	31±6	80	<0.001
R/W_B± SD	3.1±0.3	2.7±0.1	14	<0.001
(ϑ_R ± SD) (degrees)	8±2	8±1	0	0.60
(p_{max}/W_B ± SD) (m^{-2})	7100±3500	3500±900	65	<0.001

SD: standard deviation. Adapted from [29].

Table 2. Average values of geometrical and biomechanical parameters of 47 dysplastic and 36 »normal« female hips.

It seems reasonable that in hips that were assigned dysplastic, mostly due to poor coverage of the femoral head by the acetabulum the area that bears resultant hip force is smaller. So it could be concluded that in these hips the reasons for development of arthritis are mechanical in a sense that too high stress causes degeneration of the tissues and inflammation of hip joint. In other words, hip arthritis in these cases is secondary to increased contact hip stress that reflects unfavorable geometry of the hips and pelvis.

It can be seen from Table 2 that the parameters for the above example assessed from nomograms were the average parameters of the »normal« hips. The peak stress obtained by using the nomograms (3300 m^{-2}) differs from the average hip stress calculated by the computer program 3500±900 m^{-2} (Table 2) for about 6%. Yet it should be considered that the value 3500 m^{-2} was not obtained by calculating stress from the average parameters presented in Table 2 but by averaging stresses of hips included in the study.

5.3. »Normal« hips

Secondary arthritis caused by hip dysplasia represents a minor part in the population of hip arthritis, so the question was posed whether the hips with diagnosis »dysplasia coxae« are in fact the extreme subpopulation of hips with too high hip stress and that a considerable number of hips with diagnosis »idiopathic hip arthritis« are in fact poorly described hips with too high hip stress. This question has already been addressed previously and the negative answer given by the thorough study of large cohort [16] brought evidence against the mechanical hypothesis.

http://dx.doi.org/10.5772/59976

However, decisive and transparent description of dysplastic hips by the HIPSTRESS method was an indication to reconsider the validity of the mechanical hypothesis also in idiopathic osteoarthritis.

As it was expected that the differences between the diseased and »normal« hips would in the population considering hips with idiopathic osteoarthritis be smaller, another question was rised, i.e. which hips can be considered »normal«. To better define the »normal« hips, a more thorough study was performed considering asymptomatic hips [30]. The population considered in the previous study [27] was expanded to 164 female and 42 male »normal« hips. In the female group the subjects' age ranged from 18 to 86, median 54. In the male group the subjects' age ranged from 23 to 82, median 54.

Figure 7 shows the dependence of the peak hip stress on the age of the subject. It can be seen that in the female and in the male population the values of peak stress were scattered over a large interval (between 2000 and 6000 m^{-2} in the female population and between 1500 and 4000 m^{-2} in the male population). With increasing age, the lower bound of the peak stress values remained more or less the same while the upper bound diminished. There were no »normal« old subjects with high hip stress. The average value of peak hip stress decreased with age. It was interpreted that hips that seem »normal« at young age (are asymptomatic) but have high peak stress are removed from the population of »normal« hips in the middle or old age due to development of early hip arthritis, thereby leaving in the »normal« population only hips with low peak stress. With aims at healthy ageing and higher lifespan it would be more appropriate to consider hip as »normal« only if it is asymptomatic at old age. According to the results presented in Figure 7, the appropriate value for »healthy« hips asymptomatic at 80 years would be about 2000 m^{-2} in both sexes. Most importantly, it was concluded that when comparing populations, special care should be taken with regard to the age of the subjects. In the study of Brinckmann et al. (1981) [16] the subjects in the group of »normal« hips were on the average younger than the subjects in the group of hips with arthritis, so some hips that were regarded as »normal« could have at the mathching age pertained to the group of hips with arthritis. These arguments encouraged reconsideration of validation of the mechanical hypotehsis also for hips with idiopathic arthritis.

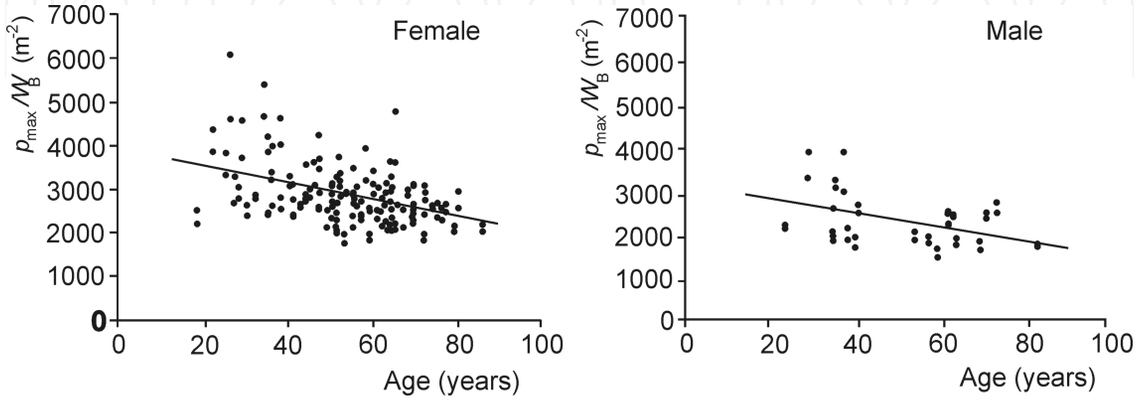

Figure 7. Peak contact hip stress in the population of »normal« hips in dependence on subject's age. Adapted from [30].

6. Comparison of »normal« hips and hips with idiopathic arthritis

The mechanical hypothesis for the primary hip arthritis was validated by considering a group of 431 female patients who underwent total hip replacement [31]. Patients for whom secondary causes for hip arthritis were known were excluded (90 patients with rheumatoid or psoriatic arthritis, avascular necrosis, slipped capital femoral epiphysis, dysplasia of the hip or lower extremity fracture). Radiograms of hips and pelvis of 92 of the patients that were taken years before the operation for various reasons (back pain, discrete pain in the hips or minor injury to the pelvis) were retrieved from the archives, 65 of these radiograms were of required quality and showed hips without considerable joint space narrowing (mean width 3 mm), large osteophytes, subchondral cysts or acetabular protrusion. Three of these patients could not be located and one did not consent to participate in the study while two patients reported a fracture of the lower extremity during childhood. The final analysis was performed on 59 radiograms of hips with no or only initial stage of hip arthritis. The side of arthritis that developed later was determined from medical records on arthroplasty. Geometrical and biomechanical parameters were assessed. There were 22 female patients with unilateral hip arthritis (aged 45 to 79 years, median 69 years) and 37 female patients with bilateral disease (aged 50 to 80 years, median 68 years). In the population with unilateral disease, the parameters of the hips with arthritis were compared to the respective parameters of the contralateral hips with no sign of degenerative process. In the population with bilateral disease, the parameters of hips with earlier implantation of hip endoprosthesis were compared to the respective parameters of contralateral hips with later implementation of hip endoprosthesis.

	Hips with arthritis (22)	Normal hips (36)	Difference (%)	p
(C ± SD) (cm)	6.4±1.1	6.5±1.0	-2	0.50
(H ± SD) (cm)	15.7±0.8	15.8±0.8	-1	0.18
(x ± SD) (cm)	1.1±0.9	1.2±0.9	-9	0.41
(z ± SD) (cm)	6.7±0.6	6.8±0.5	-1	0.07
(r ± SD) (cm)	2.6±1.5	2.6±1.4	0	
(ϑ_{CE}±SD) (degrees)	33.5±7.1	35.2±7.3	5	0.03
R/W_B± SD	2.61±0.21	2.58±0.21	1	0.21
(ϑ_R ± SD) (degrees)	7.8±1.3	7.9±1.1	-1	0.47
(p_{max}/W_B ± SD) (m^{-2})	2440±490	2320±210	5	<0.001

SD: standard deviation. Adapted from [31].

Table 3. Average values of geometrical and biomechanical parameters of 22 female hips with arthritis and 22 contralateral »normal« hips.

http://dx.doi.org/10.5772/59976

	Hips with earlier arthritis (37)	Contralateral hips with later arthritis (37)	Difference (%)	p
(C ± SD) (cm)	6.5±10.9	6.5±0.9	0	0.65
(H ± SD) (cm)	15.4±0.8	15.4±0.9	0	0.22
(x ± SD) (cm)	1.4±0.7	1.1±0.8	23	0.05
(z ± SD) (cm)	6.5±0.5	6.7±0.5	3	0.01
(r ± SD) (cm)	2.6±1.8	2.6±1.7	0	0.09
(ϑ_{CE}±SD) (degrees)	35.1±8.3	36.7±8.5	-4	0.005
R/W_B± SD	2.59±0.17	2.54±0.17	2	0.005
(ϑ_R ± SD) (degrees)	7.8±1.3	7.9±1.1	-1	0.016
(p_{max}/W_B ± SD) (m^{-2})	2540±550	2350±490	81	<0.001

SD: standard deviation. Adapted from [31].

Table 4. Average values of geometrical and biomechanical parameters of 37 female hips with bilateral arthritis. The hips in which arthritis developed earlier were compared with the hips in which arthritis developed later.

These results provided evidence in favor of the mechanical hypothesis by showing that hips with idiopathic arthritis had statistically significantly higher peak hip stress than contralateral asymptomatic hips (Table 3) and that higher peak hip stress meant clinically worse result (Table 4). As it is clear that hips with small centre-edge angle (smaller than 20 degrees) have very high peak stress and that hips with rather large centre-edge angle (larger than 35 degrees) have low hip stress, in hips in between these values the other geometrical parameters can importantly influence the stress. In standard procedures which are often based on the centre-edge angle and the shape of the femoral head, these hips are not recognized as dysplastic, however, a combination of high and wide pelvis, laterally small extension of the greater trochanter and small radius of the femoral head may result in high hip stress. It is therefore indicated that rough estimation of stress on the basis of the visual experience should be supported by actually calculating stress.

7. Hip stress gradient index as a relevant biomechanical parameter

It was suggested [23] that hip stress gradient index is an appropriate parameter to assess hip dysplasia. As described above, the hip stress gradient index describes the derivative of the hip stress with respect to medial direction, at the lateral acetabular rim. If the hip stress increases in the medial direction at the lateral rim, G_p is negative, while if it decreases, it is positive.

A population of hips diagnosed with hip dysplasia according to standard criteria and a group of »normal« hips were examined for the hip stress gradient index [23]. The respective populations consisted of 56 dysplastic hips (9 male and 47 female) and 146 »normal« hips. Figure

3 shows a dependence of hip stress gradient index on the centre-edge angle for both populations of hips. It can be seen that for small centre edge angles G_p is positive, but it diminishes with increasing centre-edge angle. The parameter G_p changes sign at the centre-edge angle approximately equal 20 degrees. The scattering of G_p shows that parameters besides the centre-edge angle are also important; the scattering is larger for smaller centre-edge angles. The difference between the average values of G_p pertaining to the group of dysplastic hips ($1.48.10^5$ m^{-3}) and to the group of normal hips ($-0.44.\ 10^5$ m^{-3}) as assessed by the t-test was statistically signifficant ($p<0.001$).

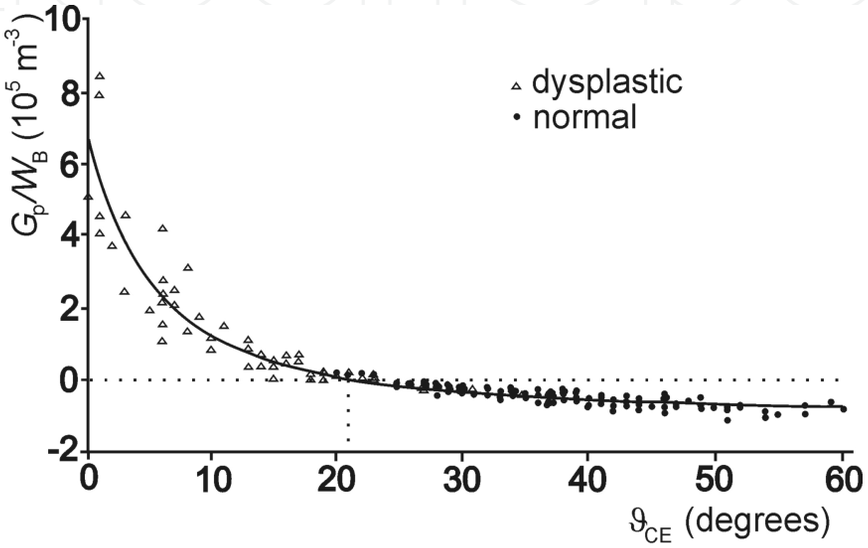

Figure 8. Hip stress gradient index in dependence on centre-edge angle for dysplastic and for »normal« hips. Adapted from [23].

An independent group of 45 dysplastic and »normal« hips was assessed by the Harris hip score for pain, performance and mobility [23]. A statistically significant correlation was found between the Harris hip score and the hip stress gradient index ($\varrho = -0.426$, $p<0.01$). Hip stress gradient index was tested as a criterion for hip dysplasia in these hips. The hips were divided into two groups. The group with positive G_p (16 hips) and the group with negative G_p (29 hips). For comparison, the method for estimating hip dysplasia based on the centre-edge angle was used; the hips with centre-edge angle smaller than 20 degrees were considered dysplastic. There were 10 such hips and 35 hips with centre-edge angle larger than 20 degrees. The difference in Harris hip score between the corresponding groups of dysplastic and »normal« hips were estimated by a non-parametrical statistical test (Kolmogorov-Smirnov test). By considering G_p as the criterion, the difference between the two groups was found statistically significant ($p = 0.031$) while by considering the centre-edge angle as a criterion, the difference was not statistically significant ($p=0.233$). In this group of hips the hip stress gradient index proved a better parameter to predict the Harris hip score than the centre-edge angle [23]. As the hip stress gradient index reflects the distribution of stress over the weight bearing area, it was suggested due to these results that G_p may prove complementary or even more important than he peak stress in assessment of the risk for hip arthritis development.

http://dx.doi.org/10.5772/59976

8. Hip stress gradient index as a relevant biomechanical parameter in hips that were in childhood subjected to Legg-Calve-Perthes disease

Legg-Calve-Perthes disease may considerably affect the development of the hip resulting in deformed femur and acetabulum (Figure 1, right hip). As the risk for arthritis development is increased in hips that were in the childhood subjected to Legg-Calve-Perthes disease, it was of interest to determine biomechanical parameters in these hips and compare them with the corresponding parameters of »normal« hips. The group of contralateral asymptomatic hips with no aparent deformities were considered as the group of »normal« hips. 259 patients were initially considered in the study [26]. 167 patients (64.5%) attended a control examination which included measurement of height and weight of the patient. 3 patients were omitted for missing X-ray pictures from the time of the disease, 19 patients were omitted due to bilateral disease, 3 patients were omitted due to absence of radiograms at the follow-up, 5 patients were omitted due to inadequate X-ray pictures and 2 patients were omitted as they already had a hip prosthesis implanted due to hip arthritis. The final cohort included 135 patients. 24 hips were female (17.8%) and 111 hips were male (82.2%). The mean age at follow-up was 32.5 (20.6 – 47.6) years and the mean body mass index (BMI) at follow-up was 26.7 (18 – 38) kg/m^2.The mean time interval between treatment and follow up was 25.6 (14.5 – 34.5) years. As the body weight was measured at the control examination it was possible to determine both, the normalized biomechanical parameters and the »whole« parameters.

Average±SD	Hips subjected to Legg-Calve-Perthes disease in childhood	Normal (contralateral asymptomatic) hips	Approximate difference (%)	p	Statistical power (1-β)
ϑ_{CE}(degrees)	24.1±9.7	32.9±6.5	-31	$<10^{-8}$	1.00
r (cm)	2.84±0.49	2.43±0.22	15	$<10^{-8}$	1.00
R (N)	2099±474	2100±472	0	0.936	< 0.20
R/W_B	2.59±0.23	2.59±0.20	0	0.797	< 0.20
θ (degrees)	24.3±13.9	13.9±7.0	55	$<10^{-8}$	1.00
p_{max} (MPa)	2.30±0.88	2.28±0.64	0	0.647	0.27
p_{max}/W_B (m^{-2})	2932±945	2911±773	0	0.762	< 0.20
G_p(MPa/m)	4.46±43.55	-29.45±29.69	>100	$<10^{-8}$	1.00
G_p/W_B (m^{-3})	4334±51011	-37959±35848	>100	$<10^{-8}$	1.00
A_F (cm^2)	12.2±3.0	11.3±2.4	7	2.10^{-4}	0.94
ϑ_F (degrees)	90.2±22.7	108.7±13.5	-18	$<10^{-8}$	1.00

Table 5. Average values of geometrical and biomechanical parameters of hips that were in the childhood subjected to Legg-Calve-Perthes disease and "normal" (contralateral) hips. The probabilities (p-value) were calculated with the two-tailed paired t-test and post-hoc statistical power (1-β) calculated for $\alpha = 0.05$ and sample size N = 135. Statistical power was 1 also for $\alpha = 10^{-8}$ for the variables that yielded differences with statistical significance $p < 10^{-8}$. Adapted from [26].

It can be seen in Table 5 that there were no statistically significant differences between the two groups in resultant hip force and peak contact hip stres (normalized and »whole«). The centre-edge angle was considerably and statistically significantly more favorable in »normal« hips, however, the hips that were in the childhood subjected to the disease had developed a considerably and statistically significantly larger femoral head which compensated the effect of the smaller centre-edge angle. Figure 9 shows that in the group of »normal« hips (red dots) the radii were smaller and uniformly distributed over the interval of centre-edge angles. The lower bound of this interval was approximately 20 degrees as previously acknowledged to be a criterion for hip dysplasia. The test group extended also below this interval, but here the radii were considerably larger. This effect overcompensated the load bearing area which was (statistically significantly) larger in the test group although the centre-edge angle was smaller (Table 5).

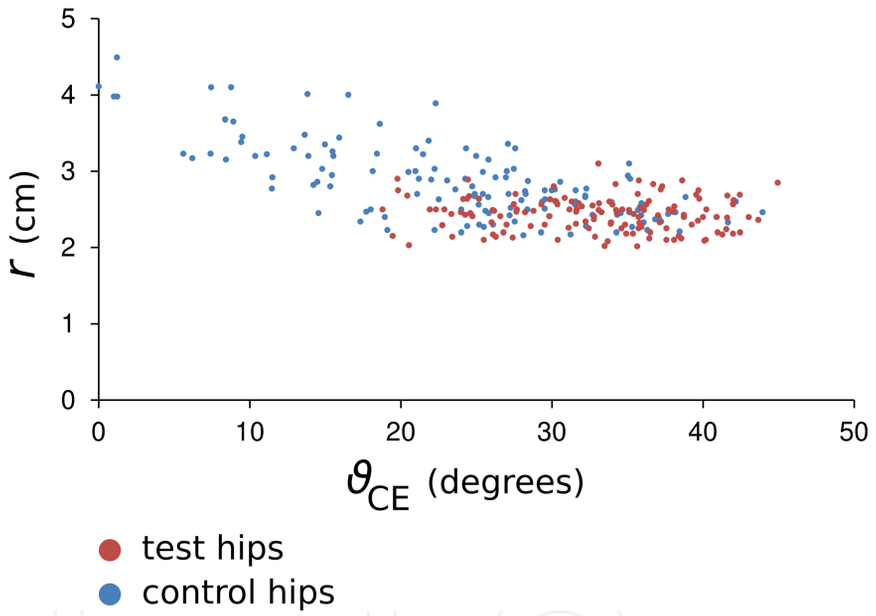

Figure 9. Interdependence between the radius of the femoral head and the centre-edge angle in hips that were in childhood subjected to Legg-Calve-Perthes disease (test group) and contralateral "normal" hips (control group). From [26].

In the hips that were in childhood subjected to Legg-Calve-Perthes disease the resultant hip force and the peak stress did not show differences while the load bearing area was more favorable, however, the stress pole was located considerably and statistically significantly more laterally than in the control group which was reflected also in the difference in the functional angle (Table 5). Most importantly, the biomechanical parameter that showed the difference between the two groups in favor of »normal« hips was the hip stress gradient index. The respective differences in the normalized and the »whole« parameter were considerable (larger than 100%) and statistically very significant (Table 5). The cohort was large enough (with high statistical power at very small probabilities) to render the above results decisive.

http://dx.doi.org/10.5772/59976

Figure 10 shows dependence of hip stress gradient index on the centre-edge angle (A) and on the radius of the femoral head (B). Almost all »normal« hips are confined within the boundaries of radii smaller than 3 cm, centre-edge angles larger than 20 degrees and negative hip stress gradient indexes while the hips that were in childhood subjected to Legg-Calve-Perthes disease extended beyond these boundaries (to larger radii, smaller centre-edge angles and positive hip stress gradient indexes). But there were also many hips from the test group that fitted well within the group of »normal« hips showing successful recovery from the disease in the childhood.

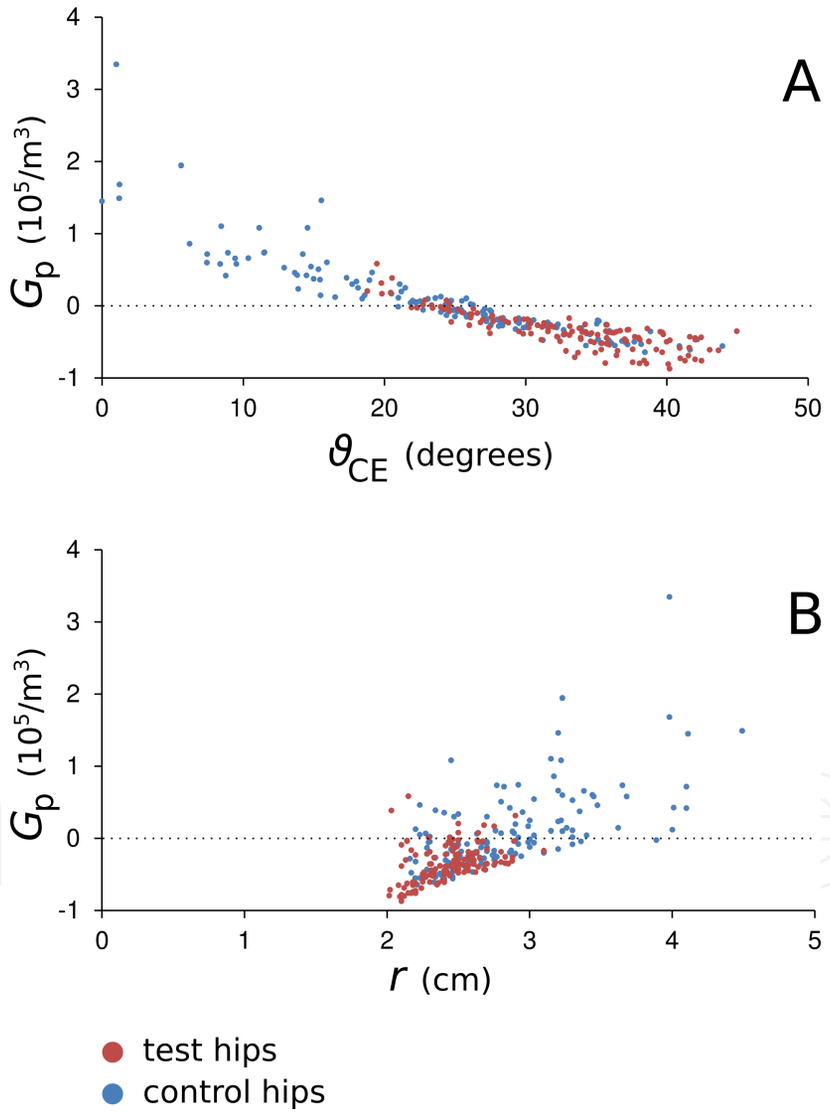

Figure 10. Dependence of the hip stress gradient index on the centre-edge angle (A) and on the radius of the femoral head (B) in hips that were in childhood subjected to Legg-Calve-Perthes disease (test group) and contralateral "normal" hips (control group). From [26].

9. Conclusion

Method HIPSTRESS proved useful in contributing evidence in favor of mechanical hypothesis stating that long lasting unfavorable stress distribution is an etiological factor in development of hip arthritis. The mathematical model for resultant hip force contains the relevant choice of muscles and appropriate scaling of their attachment points that emphasize the individual geometry. The mathematical model is not simple in its derivation, however, it is expressed by transparent and almost analytical solution. The computer program and nomograms enable medical doctors and students to use the mathematical models without extensive mathematical skills. Knowing the geometrical parameters the resultant hip force and the peak stress can be determined within minutes. It is shown above that peak hip stress showed differences between dysplastic and normal hips and between hips with idiopathic arthritis and normal hips. However in dysplastic hips also the hip stress gradient index was less favorable (larger), so it is unclear which of these parameters is the most relevant to estimate the risk for development of hip arthritis. The role of hip stress gradient index is emphasized also by the study of hips that were in childhood subjected to Legg-Calve-Perthes disease since in these hips the resultant hip force and the peak stress were not elevated. Further studies are needed to obtain answer to this question. The method could be supported by using improved imaging of hips (three dimensional data on muscle attachment points) and refined by considering particularities of diseases (such as nonsphericity of femoral head after the Legg-Calve-Perthes disease). Most importantly, the hypothesis involving macroscopic hip stress distribution should be connected to molecular mechanisms underlaying cartilage deterioration and onset and spreading of inflammation.

The criteria for biomechanical measures suggested by R.A. Brand [32] are that they (a) should be accurate and reproducible, (b) the measuring technique must not significantly alter the function it is measuring, (c) it should exhibit reasonable stability, (d) the measure should not be directly observable by the skilled clinician, (e) it should be independent of mood, motivation or pain, (f) it must clearly distinguish between normal and abnormal, (g) it should be reported in a form analogous to some accepted clinical concept, (h) it should be cost-effective and (i) it must be appropriately validated. As a method based on physical laws the HIPSTRESS method completely fulfills the criteria (b), (c), (d), (e), (g) and (h). As for criterion (a) it is reproducible, but its accuarcy is limited by the model assumptions and by the accuracy of measurement of geometrical parameters. Further improvements should be made in these directions. Criterion (f) adresses »normal« and »abnormal«. A clear criterion can be given within the HIPSTRESS method (i.e. threshold values of biomechanical parameters such as G_p=0), however, these are based on correspondence of the parameters with clinical assessment which is also not always clear. The criterion (*i*) was implemented by validation of the HIPSTRESS method by studies of the effect of different operations on biomechanical and clinical outcome and related problems [32-57]. The strongest point of the method is low invasiveness (it uses data that were obtained for therapeutic purposes). Also, the development of the method and its use required no experiments on laboratory animals or any other material that would require burden on patients, volunteers or animals.

http://dx.doi.org/10.5772/59976

Author details

Veronika Kralj-Iglič*

Address all correspondence to: veronika.kralj-iglic@fe.uni-lj.si

Laboratory of Clinical Biophysics, Faculty of Health Sciences, University of Ljubljana, Ljubljana, Slovenia

References

[1] Wiberg G. Studies on dysplastic acetabula and congenital subluxation of the hip joint: with special reference to the complication of osteoarthritis. Acta Chir Scand Suppl. 1939; 58:7-135.

[2] Chiari K. Pelvic osteotomy in hip arthroplasty. Wien Med Wochenschr. 1953;103(38): 707–709.

[3] Salter RB. Innominate osteotomy in the treatment of congenital dislocation and subluxation of the hip. J Bone Joint Surg Br. 1961; 43(3):518–539.

[4] Pemberton PA. Pericapsular osteotomy of the ileum for treatment of congenital subluxation and dislocation of the hip. J Bone Joint Surg Am. 1965; 47(1):65–86.

[5] Chiari K. Medial displacement osteotomy of the pelvis. Clin Orthop Relat Res. 1974; 98:55–71.

[6] Salter RB, Hansson G, Thompson GH. Innominate osteotomy in the management of residual congenital subluxation of the hip in young adults. Clin Orthop Relat Res. 1984; 182:53–68.

[7] Steel HH. Triple osteotomy of the innominate bone. J Bone Joint Surg Am. 1973; 55(2):343–350.

[8] Ganz R, Klaue K, Vinh TS, Mast JW. A new periacetabular osteotomy for the treatment of hip dysplasias. Technique and preliminary results. Clin Orthop Relat Res. 1988; 232:26–36.

[9] Tonnis D. Surgical treatment of congenital dislocation of the hip. Clin Orthop Relat Res.1990; (258):33–40.

[10] Brand RA, Iglic A, Kralj-Iglic V. Contact stresses in human hip: implications for disease and treatment. Hip Int. 2001; 11:117-126.

[11] Hodge WA, Fijan RS, Carlson KL, Burgess RG, Harris WH, Mann RW. Contact pressures in the human hip joint measured in vivo. Proc Natl Acad Sci USA.1986; 83 (9): 2879-2883.

[12] Brown TD, DiGioia AM 3rd. A contact-coupled finite element analysis of the natural adult hip. J Biomech. 1984; 17(6):437-448.

[13] Crowninshield RD, Johnston RC, Andrews JG, Brand RA. A biomechanical investigation of the human hip. J Biomech. 1968; 11:75-77.

[14] Pauwels F. Biomechanics of the normal and diseased hip: Theoretical foundations, technique, and results of treatment, 276. Berlin: Springer-Verlag; 1976.

[15] Legal H, Reinecke M, Ruder H. Zur biostatischen analyse des hüftgelenks III. Z Orthop Ihre Grenzgeb. 1980; 118(5):804-15.

[16] Brinckmann P, Frobin W, Hierholzer E. Stress on the articular surface of the hip joint in healthy adults and persons with idiopathic osteoarthrosis of the hip joint. J Biomech. 1981; 14:149–156.

[17] Hadley NA, Brown TD, Weinstein SL. The effects of contact pressure elevations and aseptic necrosis on the long-term outcome of congenital hip dislocation. J Orthop Res. 1990; 8:504-513.

[18] Maxian TA, Brown TD, Weinstein SL. Chronic stress tolerance levels for human articular cartilage: Two nonuniform contact models applied to long-term follow-up of CDH. J Biomech. 1995; 28:159-166.

[19] Iglic A, Srakar F, Antolic V, Kralj Iglic V, Batagelj V. Mathematical analysis of Chiari osteotomy. Acta Orthop Iugosl. 1990; 20:35-39.

[20] Ipavec M, Brand RA, Pedersen DR, Mavcic B, Kralj-Iglic V, Iglic A. Mathematical modelling of stress in the hip during gait. J Biomech. 1999; 32:1229-1235.

[21] Dostal WF, Andrews JG. A three dimensional biomechanical model of hip musculature. J. Biomehanics. 1981; 14:803-812.

[22] Johnston RC, Brand RA, Crowninshield RD. Reconstruction of the Hip. J. Bone and Joint Surg. 1979; 61A:639-652.

[23] Pompe B, Daniel M, Sochor M, Vengust R, Kralj-Iglic V, Iglic A. Gradient of contact stress in normal and dysplastic human hips. Med Eng Phys. 2003; 25:379-385.

[24] Kralj-Iglic V, Dolinar D, Ivanovski M, List I, Daniel M. Role of biomechanical parameters in hip osteoarthritis and avascular necrosis of femoral head. Applied Biological Engineering - Principles and Practice, Naik GR (Ed.), InTech, DOI: 10.5772/30159; 2012.

[25] Rijavec B, Kosak R, Daniel M, Kralj-Iglic V, Dolinar D. Effect of cup inclincation on predicted stress-induced volumetric wear in total hip replacement. Comput Meth Biomech Biomed Eng. 2014; DOI: 10.5772/30159.

[26] Kocjancic B, Molicnik A, Antolic V, Mavcic B, Kralj-Iglic V, Vengust R. Unfavorable hip stress distribution after Legg-Calve-Perthes syndrome: a 25-year follow-up of 135 hips. J Orthop Res. 2014; 32:8-16.

[27] Daniel M, Antolic V, Iglic A, Kralj Iglic V. Determination of contact hip stress from nomograms based on mathematical model. Med Eng Phys. 2001; 23:347-357.

[28] Kersnic B, Iglic A, Kralj-Iglic V, Srakar F, Antolic V. Increased incidence of arthrosis in female population could be related to femoral and pelvic shape. Arch Orthop Trauma Surg. 1997; 116:345-347.

[29] Mavcic B, Pompe B, Antolic V, Daniel M, Iglic A, Kralj-Iglic V. Mathematical estimation of stress distribution in normal and dysplastic human hips. J Orthop Res. 2002; 20:1025-1030.

[30] Mavcic B, Slivnik T, Antolic V, Iglic A, Kralj-Iglic V. High contact hip stress is related to the development of hip pathology with increasing age. Clin Biomech. 2004; 19:939-943.

[31] Recnik G, Kralj-Iglic V, Iglic A, Antolic V, Kranberger S, Vengust R. Higher peak contact hip stress predetermines the side of hip involved in idiopathic osteoarthritis. Clin Biomech. 2007; 22:1119–1124.

[32] Brand RA. Can biomechanics contribute to clinical orthopaedic assessments? Iowa Orthop J 1989; 9:61-64.

[33] Pompe B, Antolic V, Mavcic B, Iglic A, Kralj-Iglic V. Hip joint contact stress as an additional parameter for determining hip dysplasia in adults: Comparison with severin's classification. Med Sci Monit. 2007; 13:CR215-219.

[34] Kristan A, Mavcic B, Cimerman M, Iglic A, Tonin M, Slivnik T, Kralj-Iglic V, Daniel M. Acetabular Loading in Active Abduction. IEEE T Rehabil Eng. 2007; 15:252-275.

[35] Daniel M, Dolinar D, Herman S, Sochor M, Iglic A, Kralj-Iglic V. Contact stress in hips with osteonecrosis of the femoral head. Clin Orhop Rel Res. 2006; 447:92-99.

[36] Kralj M, Mavcic B, Antolic V, Iglic A, Kralj-Iglic V. The Bernese periacetabular osteotomy: clinical, radiographic and biomechanical 7-15 year follow-up in 26 hips. Acta Orthop. 2005; 76:833-840.

[37] Daniel M, Iglic A, Kralj-Iglic V. The shape of acetabular cartilage optimizes hip contact stress distribution. J Anat. 2005; 207:85–91.

[38] Daniel M, Iglic A, Kralj-Iglic V, Konvickova S. Computer system for definition of the quantitative geometry of musculature from CT images. Comput Methods Biomech Biomed Engin. 2005; 1:25-29.

[39] Kosak R, Antolic V, Pavlovcic V, Kralj-Iglic V, Milosev I, Vidmar G, Iglic A. Polyethylene wear in total hip prostheses: the influence of direction of linear wear on

volumetric wear determined from radiographic data. Skeletal Radiol. 2003; 23: 679-686.

[40] Dolinar D, Antolic V, Herman S, Iglic A, Kralj-Iglic V, Pavlovcic V. Influence of contact hip stress on the outcome of surgical treatment of hips affected by avascular necrosis, Arch Orthop Trauma Surg. 2003; 123:509-513.

[41] Daniel M, Sochor M, Iglic A, Kralj-Iglic V. Hypothesis of regulation of hip joint cartilage activity by mechanical loading. Med Hypotheses. 2003; 60: 936-937.

[42] Herman S, Jaklic A, Herman S, Iglic A, Kralj-Iglic V. Hip stress reduction after Chiari osteotomy. Med Biol Eng Comput. 2002; 40: 369-375.

[43] Iglic A, Kralj-Iglic V, Daniel M, Macek-Lebar A. Computer determination of contact stress distribution and size of weight bearing area in the human hip joint. Comp Methods Biomed. Eng. 2002; 5: 185-192.

[44] Vengust R, Daniel M, Antolic V, Zupanc O, Iglic A, Kralj-Iglic V. Biomechanical evaluation of hip joint after Salter innominate osteotomy: a long-term follow-up study. Arch Orthop Trauma Surg. 2001; 121: 511-516.

[45] Iglic A, Daniel M, Kralj-Iglic V, Antolic V, Jaklic A. Peak hip-joint contact stress in male and female populations. J Musculoskeletal Res. 2001; 5: 17-21.

[46] Zupanc O, Antolic V, Iglic A, Jaklic A, Kralj-Iglic V, Stare J, Vengust R. The assessment of contact stress in the hip joint after operative treatment for severe slipped capital femoral epiphysis. Int Orthop. 2001; 25:9-12.

[47] Antolic V, Srakar F, Iglic A, Kralj-Iglic V, Zaletel-Kragelj L, Macek-Lebar A. Changes in configuration of the hip due to Chiari osteotomy. Int Orthop. 1996; 4:183-186.

[48] Iglic A, Antolic V, Srakar F, Kralj-Iglic V, Macek-Lebar A, Brajnik D. Biomechanical study of various greater trochanter positions. Arch Orthop Trauma Surg. 1995; 114:76-78.

[49] Antolic V, Iglic A, Herman S, Srakar F, Kralj-Iglic V, Macek-Lebar A, Stanic U. The required and the available abductor force after operative changes in pelvic geometry. Acta Orthop Belg. 1994; 60:374-377.

[50] Iglic A, Kralj-Iglic V, Antolic V. Reducing of stress in the articular surface of the hip joint after shifting the upper part of the body towards the painful hip. Acta Chir Orthop Traum Cech. 1994; 61:268-270.

[51] Iglic A, Kralj-Iglic V, Antolic V, Srakar F, Stanic U. Effect of the periacetabular osteotomy on the stress on the human hip joint articular surgace. IEEE Trans Rehab Engr. 1993; 1:207-212.

[52] Iglic A, Antolic V, Srakar F. Biomechanical analysis of various operative hip joint rotation center shifts. Arch Orthop Trauma Surg. 1993; 112:124-126.

[53] Iglic A, Srakar F, Antolic V. The influence of the pelvic shape on the biomechanical status of the hip. Clin Biomech. 1993; 8:223-224.

[54] Srakar F, Iglic A, Antolic V, Herman S. Computer simulation of the periacetabular osteotomy. Acta Orthop Scand. 1992; 63:411-412.

[55] Kosak R, Kralj-Iglic V, Iglic A, Daniel M. Polyethylene wear is related to patient-specific contact stress in THA. Clin Orthop Rel Res. 2011; 469:3415-3422.

[56] Mavcic B, Daniel M, Antolic V, Iglic A, Kralj-Iglic V. Contact hip stress measurements in orthopaedic clinical practice. In: Biomechanics: Principles, Trends and Applications. Ed: Levy JH. Nova Science Publishers; (2010). p281-294.

[57] Debevec H, Pedersen DR, Iglic A, Daniel M. One-legged stance as a representative static body position for calculation of hip contact stress distribution in clinical studies. J Appl Biomech. 2010; 26:522-525.

IntechOpen